Available online at www.sciencedirect.com
SCIENCE DIRECT®
Journal of Structural Biology 148 (2004) 268–278
Journal of Structural Biology
www.elsevier.com/locate/yjsbi

Assembly of collagen into microribbons: effects of pH and electrolytes

Fengzhi Jiang[a], Heinrich Hörber[b], Jonathon Howard[c], Daniel J. Müller[a,*]

[a] *Biotechnological Center, University of Technology Dresden, 01062 Dresden, Germany*
[b] *European Molecular Biological Laboratory, 69112 Heidelberg, Germany*
[c] *Max-Planck-Institute of Molecular Cell Biology and Genetics, 01307 Dresden, Germany*

Received 5 February 2004
Available online 27 August 2004

Abstract

Collagen represents the major structural protein of the extracellular matrix. Elucidating the mechanism of its assembly is important for understanding many cell biological and medical processes as well as for tissue engineering and biotechnological approaches. In this work, conditions for the self-assembly of collagen type I molecules on a supporting surface were characterized. By applying hydrodynamic flow, collagen assembled into ultrathin (~3 nm) highly anisotropic ribbon-like structures coating the entire support. We call these novel collagen structures microribbons. High-resolution atomic force microscopy topographs show that subunits of these microribbons are built by fibrillar structures. The smallest units of these fibrillar structures have cross-sections of $\sim 3 \times 5$ nm, consistent with current models of collagen microfibril formation. By varying the pH and electrolyte of the buffer solution during the self-assembly process, the microfibril density and contacts formed within this network could be controlled. Under certain electrolyte compositions the microribbons and microfibers display the characteristic D-periodicity of ~65 nm observed for much thicker collagen fibrils. In addition to providing insight into the mechanism of collagen assembly, the ultraflat collagen matrices may also offer novel ways to bio-functionalize surfaces.

Keywords: Atomic force microscopy; Microfibrils; Microribbons; Molecular interactions; Protein assembly

1. Introduction

Collagen represents the most abundant structural protein found in multicellular animals. Members of this family, of which more than 20 specialized collagens have been characterized, either form fibrils or other assemblies shaping and organizing the extracellular matrix (ECM).[1] This scaffold of the ECM is then functionalized by other proteins (Hohenester and Engel, 2002). Collagens receive considerable interest because they are involved in important biological functions such as tissue structuring and cell attachment (Akiyama et al., 1990; Grinnell, 2000, 2003) and in various human diseases (Kadler, 1993; Kunicki, 2002; Myllyharju and Kivirikko, 2001; Prockop, 1998, 1999), and synthetic collagen matrices (Bishop, 2000; Coombes et al., 2002; Guidry and Grinnell, 1985; Lee et al., 2001) serve as platforms for cell biological and tissue engineering applications. Furthermore, collagen is frequently used to coat non-biological surfaces thereby enhancing biocompatibility (Coombes et al., 2002; Lee et al., 2001; Lloyd, 2002) or to pattern functionalized surfaces (Demers et al., 2002; Lee et al., 2002). Therefore, characterizing the molecular mechanisms of collagen fibril assembly is of great significance for both basic research and biotechnological applications.

Ultrastructural insights revealed by electron microscopy and X-ray diffraction indicate that tendon fibers consists of building blocks separated by average periodicities around 4–5 nm (Hulmes et al., 1981; Hulmes and Miller, 1981; Orgel et al., 2001; Prockop and Fertala,

* Corresponding author. Fax: +49 351 463 40342.
E-mail address: mueller@mpi-cbg.de (D.J. Müller).

[1] *Abbreviations used:* AFM, atomic force microscope; ECM, extracellular matrix; FWHM, full width half maximum; *n*, number; SD, standard deviation.

1047-8477/$ - see front matter © 2004 Elsevier Inc. All rights reserved.
doi:10.1016/j.jsb.2004.07.001

1998; Squire and Freundlich, 1980). From these results models of collagen assembling into microfibrils could be developed. In a first step, three peptide chains of collagen I wind into a triple-helical collagen molecule of ~300 nm in length and ~1.5 nm in diameter (Kadler et al., 1996). After this, it was suggested, that five of these collagen molecules form one microfibril (Hulmes, 2002; Orgel et al., 2001; Ottani et al., 2002). The microfibril cross-section of five stranded microfibrils exhibit a dimension of $\sim 3 \times 5$ nm, which is consistent with current models suggesting them as building blocks of larger fibrils.

Atomic force microscopy (AFM) has also provided important insights into the collagen structure. An advantage of AFM over electron microscopy is that it can be used to investigate biological systems in aqueous solution, thereby preserving their physiological conformations, and functions (Drake et al., 1989). At the same time, the high signal-to-noise ratio, superior to any other microscopic technique, can permit resolution of surface structural details down to <1 nm (Engel and Müller, 2000). AFM has been used to study collagen assembly and network formation in different types of biological systems (Bigi et al., 1997; Jurvelin et al., 1996; Marshall et al., 2001; Meller et al., 1997; Raspanti et al., 2001; Thalhammer et al., 2001), dynamic process associated with enzymatic collagen degradation (Lin et al., 1999; Sun et al., 2000), and the interaction of collagens with other molecules such as proteoglycans (Chen and Hansma, 2000; Raspanti et al., 1997) or the discoidin receptor (Agarwal et al., 2002). Several workers have used AFM to describe the structure of collagen polymerized in vitro (Chernoff and Chernoff, 1992), in rat tendon fiber (Raspanti et al., 2002; Revenko et al., 1994), in dentin collagen fibrils (Habelitz et al., 2002), and in bovine humeral articular cartilage (Jurvelin et al., 1996).

In this work, we characterize the self-assembly of collagen type I molecules onto a supporting surface by AFM. Collagen molecules were observed to assemble into highly anisotropic ribbon-like structures coating the entire supporting surface. These ribbon-like structures, which we call microribbons, formed a nanoscopic network. Microribbons are built by fibrillar structures with their smallest subunits exhibiting cross-sections of 3×5 nm. These dimensions are consistent with the above-mentioned model of collagen microfibril formation. It is found that adjusting the hydrodynamic flow, the electrolyte composition and the pH of the buffer solution affects the orientation, width, spacing, and assembly of collagen into microribbons.

2. Materials and methods

2.1. Sample preparation

Chemical reagents used were of analytical grade and prepared with ultrapure water (18 MΩ/cm). Solubilized bovine dermal collagen was prepared and purified as described (Bell et al., 1979), concentrated to 3 mg/ml and stored at pH ~2 and at a temperature of 4 °C. The final composition of the sample was 97% collagen type I and 3% collagen type III. As a supporting surface, a mica disc of 6.5 mm in diameter was used. After being freshly cleaved, the mica surface was flushed with a buffer solution containing collagen at a concentration of 0.1 mg/ml. The flow induced the alignment of collagen molecules on the support. After an adsorption time of 10 min, the sample was rinsed with the same buffer solution containing no collagen to remove molecules only loosely bound to the surface.

2.1.1. AFM

The AFMs (MultiMode, di-Veeco, CA, and NanoWizard, JPK Instruments, Germany) were operated in buffer solution using a fluid cell. Piezoelectric scanners had a scan range of $\sim 100 \times 100\ \mu m^2$. Oxide sharpened Si_3N_4 cantilevers having a nominal force constant of 0.09 N/m (OMCL TR400PS) were employed and purchased from Olympus (Tokyo). Imaging was performed in tapping mode at a RMS amplitude of approximately 25 nm and a drive frequency (8–9.5 kHz) close to the resonance frequency of the cantilevers mounted to the fluid cell immersed in buffer solution. All samples were prepared and imaged in buffer solution at room temperature (21 °C).

3. Results

3.1. pH dependence of collagen self-assembly

To investigate the pH influence on the collagen self-assembly, collagen molecules were adsorbed under hydrodynamic flow onto freshly cleaved mica at pH values ranging from 2.5 to 10.5 and subsequently imaged by AFM (Fig. 1). In these experiments, the electrolyte concentration of the buffer solution was kept constant at 200 mM NaCl. AFM topographs of the collagen samples (Fig. 1) demonstrated the effect of pH on the collagen assembly. At pH 2.5 (Fig. 1A) and 3.5 (Fig. 1B), the collagen molecules adsorbed onto mica as globular protrusions. It appeared that the densely packed particles were randomly distributed. They exhibited an average height of 3.2 ± 0.6 nm (means ± SD; $n = 100$), while their average width at half maximum height (FWHM) was 38.3 ± 7.0 nm (means ± SD; $n = 42$).

When adsorbed at pH 4.5, the appearance of the collagen molecules changed (Fig. 1C). The molecules assembled into elongated globules, which were of similar diameter to the particles observed between pH 2.5 and 3.5, but were several times longer. They were only weakly aligned in the direction of the hydrodynamic

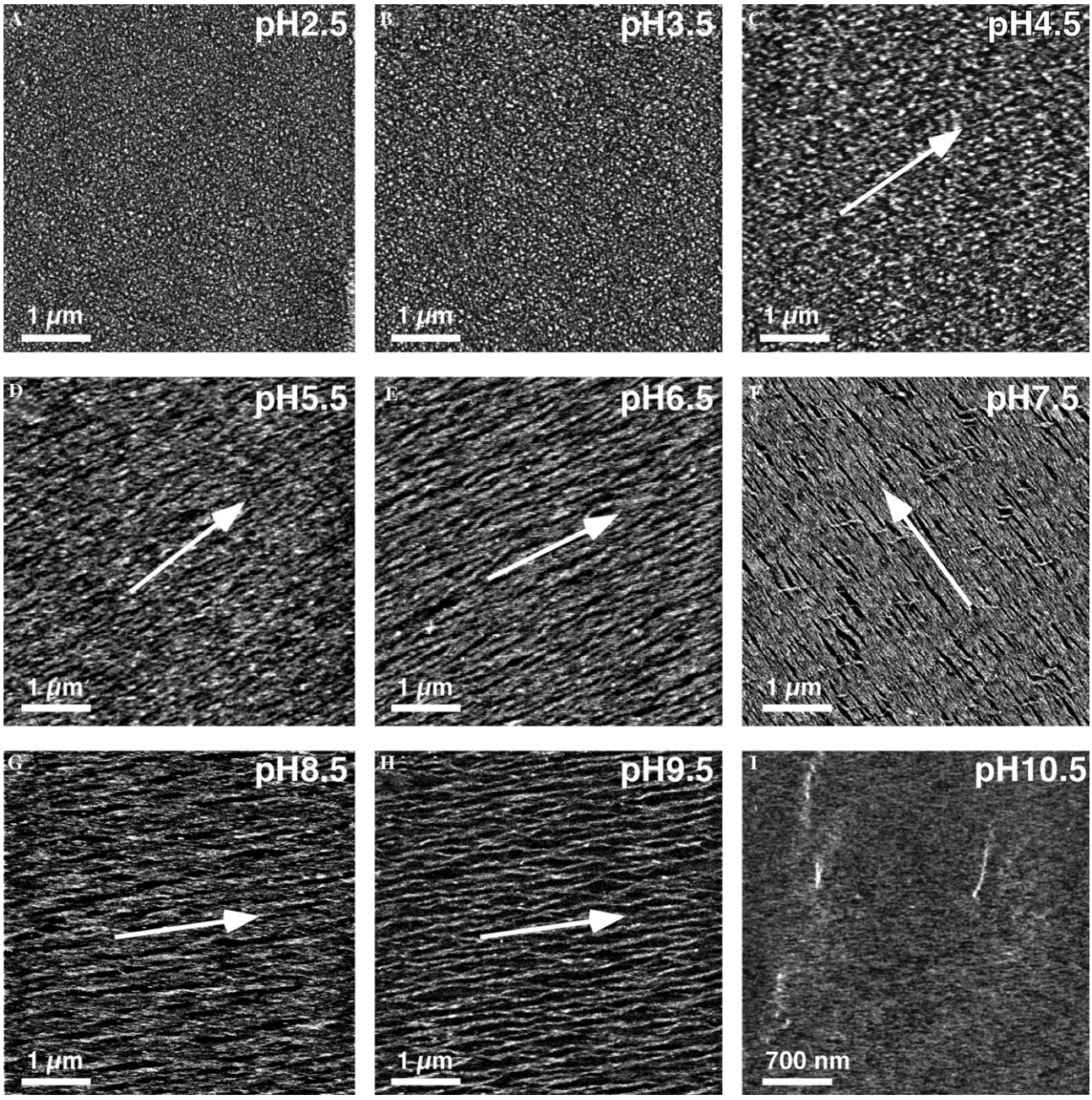

Fig. 1. Collagen self-assembly depends on pH. Being adsorbed onto mica at a pH 2.5 (A) and 3.5 (B), the collagen molecules appeared as globular protrusions. The densely packed particles were randomly distributed and exhibited an average height of 3.2 ± 0.6 nm (average ± SD; $n = 100$) above the supporting surface, while their average width at full width half maximum (FWHM) of height was about 38.3 ± 7.0 nm ($n = 42$). When adsorbed at pH 4.5, the appearance of the collagen molecules changed (C). Collagen molecules assembled into slightly elongated structures, which were a few times longer, but exhibited the same diameter as of the collagen particles observed at pH 2.5 and 3.5 (A and B). The structures observed were weakly aligned, but showed no pronounced fibrillar arrangements. When adsorbed at pH values ranging from 5.5 to 9.5 (D, pH 5.5; E, pH 6.5; F, pH 7.5; G, pH 8.5; and H, pH 9.5), the collagen molecules were observed to assemble into fibrillar structures. The fibrils formed a confluent monolayer, from which the majority of fibrils (>95%) were aligned parallel to each other. At pH 9.5, the spacing between the collagen fibrils increased slightly. At pH 10.5, a few small fragments of fibrillar structures were observed (I). The distance between these structures was too big to allow them forming contact with each other. Absorption and imaging solutions contained 200 mM NaCl and were buffered using 50 mM citric acid–NaOH (pH 2.5–5.5), and 50 mM Hepes–NaOH, pH 6.5, or 50 mM Tris–HCl, pH 7.5–10.5. Arrows point out the orientation of the fibrils. Full gray level of topographs corresponds to a vertical scale of 5 nm.

flow (Fig. 1C; arrow) and no pronounced fibrillar structures were observed. This situation changed dramatically when the pH value was adjusted to between 5.5 and 9.5 (Figs. 1D–H). Under these conditions, the mica surface was completely covered with fibrillar structures. The majority of the fibrils covering the support (>95%)

were aligned parallel to each other. Arrows point in the direction in which the collagen-containing buffer solution was guided over the supporting surface (see Materials and methods). By spotting various areas within the maximum scan range of the AFM scanner it was found that the fibrils were aligned parallel to each other over distances of more than 100 μm. To determine the spatial extent of alignment, large mica surfaces of ~20 mm in diameter were covered by the same preparation procedure. AFM topographs showed that the fibrils were aligned in the same direction over the entire surface (data not shown). This demonstrated a long-range order of the fibrils extending over several millimeters.

Upon increasing the pH from 8.5 to 9.5, the spacing between the collagen fibrils increased slightly. This resulted in the observation of fibrillar structures, which frequently formed contacts with each other at distances ranging from 300 to 1000 nm. In less densely packed regions, the height of these structures above the mica surface was 2.9 ± 0.4 nm (n = 20). In contrast, the width of the fibrillar structures varied considerably ranging from 5 to 250 nm (measured at half of maximum height). Further increasing the pH to 10.5, resulted in the adsorption of only a few elongated fragments, similar to the fibrillar structures (Fig. 1I). The distance between these structures, however, was too large for them to contact each other.

3.2. Adjusting collagen spacing by pH

In the previous section (Fig. 1) it was observed that the distance between collagen microfibrills changed significantly between pH values of 8.5 and 10.5. To study this effect in more detail, the pH of the buffer solution was increased in small steps within this range. The AFM topographs recorded showed (Fig. 2) how the average spacing between the fibrils continuously increased with the pH. At pH ranging from 8.5 (Fig. 2A) to 8.9 (Fig. 2C), the collagen fibrils formed a continuous flat layer. The spacing of the fibrils, however, increased slightly with the pH of the buffer solution.

Topographs recorded of collagen assembled at pH values ranging from 8.5 to 10.5, show a the meshlike architecture in which the collagen fibrils formed a surface-coating layer. Increasing the pH from 9.3 (Fig. 2E) to 9.5 (Fig. 2F) resulted in the adsorption of individual fibrillar structures, which were aligned parallel to each other. Only occasionally were single fibrils observed to contact their neighbors. In some cases, individual fibrils were completely isolated from each other. At pH ranges extending from pH 9.7 to 10.3 (Figs. 2G–J), all fibrils were oriented parallel parallel to each other and made no contacts with other fibrils. The spacing between the fibrils increased with increasing pH. At a pH of 10.5, only a few small fibrillar fragments were adsorbed onto the mica surface (Fig. 2K), and these had diameters between 5 and 10 nm (FWHM). At pH 10.7 no collagen molecules adsorbed onto the supporting mica surface were observed (Fig. 2L).

The effect of pH on fibril density (determined by counting the number of fibril per unit length perpendicular to the direction of alignment) is quantified in Fig. 3. The density of fibrils arranged into a monolayer is almost constant at pH values ranging from 4.5 to 8.9. At pH values above 8.9 the density decreased until, at pH >10.7, no collagen molecules adsorbed onto the surface.

3.3. Electrolyte-dependent self-assembly of collagen

To investigate the influence of electrolytes on the collagen self-assembly process, the electrolyte composition of the buffer solution was varied at a constant pH 7.5 (Fig. 4). The collagen molecules assembled into fibrils under all conditions tested at neutral pH. The electrolyte, however, influenced the organization of the fibrils. Fibrils assembled in 10 mM $MgCl_2$ were aligned parallel to each other (indicated by arrow) and exhibited protrusions (Fig. 4A; circles). These protrusions exhibited an average diameter of 35.7 ± 7.8 nm (n = 20) and a height of 3.5 ± 0.4 nm (n = 20) above the fibrils. Similar protrusions were also seen in 50 mM NaCl (Fig. 4B). In this case, however, the protrusions (ellipses) were elongated with an orientation (dotted arrow) of 55 ± 5° (n = 50) relative to that of the fibrils. On further increasing the NaCl concentration to 100 mM, the protrusions (ellipses) merged to form an incomplete second fibrillar layer (dotted arrow) on top of the layer of fibrils directly attached to the mica surface (Fig. 4C). The second layer made an angle of 58 ± 5° (n = 50) relative to the underlying fibrils. When the NaCl concentration was increased to 200 mM (Figs. 1 and 4E), the second layer of fibrils almost disappeared. In this condition, holes of diameter 20–200 nm and length 50–500 nm formed in the monolayer. Addition of 5 mM $MgCl_2$ caused these holes to almost completely disappear, resulting in a nearly close-packed monolayer of collagen fibrils (Fig. 4E).

3.4. Potassium has a profound influence on the collagen assembly

Exchanging NaCl with KCl resulted in a dramatic change in the appearance of the fibrillar structures. At 50 and 100 mM KCl, the fibrils in the monolayer were not strictly parallel to each other (Figs. 4F and G). Although, the fibrils had an overall orientation, they appeared somehow woven and twisted around each other. Accordingly, the average thickness of the resulting layers increased slightly to 3.2 ± 0.4 nm (n = 22). Increasing the KCl concentration to 200 mM resulted in a monolayer of similar appearance (Fig. 4H). Interestingly, the modulation along the axis of fibril exhibited a peri-

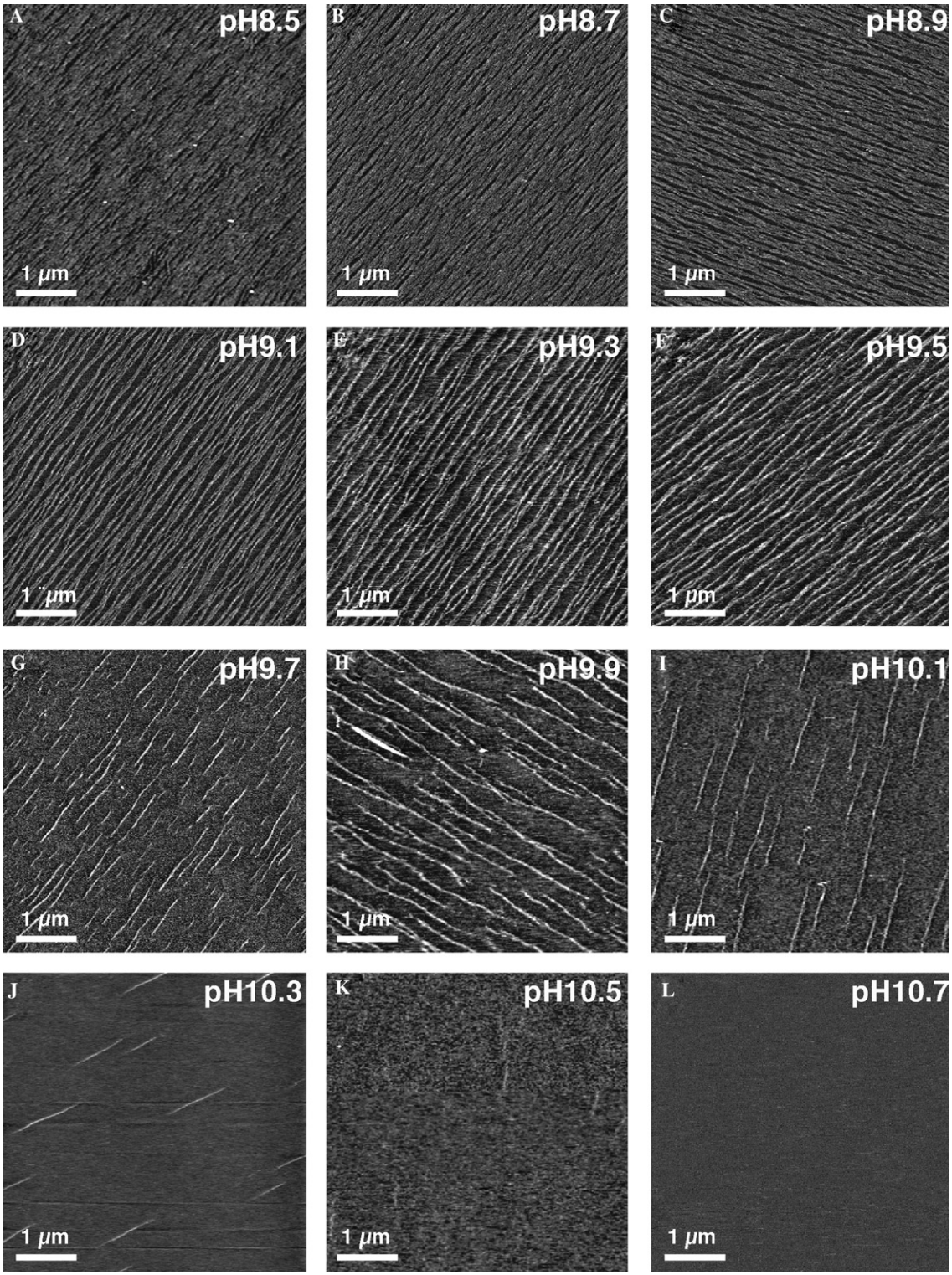

Fig. 2. Adjusting the collagen spacing by pH. In the range of pH 8.5–8.9 (A, pH 8.5; B, pH 8.7; and C, pH 8.9), parallel aligned collagen microfibrils formed a continuous monolayer. The spacing between the fibrils increased with the pH. At pH 9.1 (D), the spacing between fibrils was sufficient to observe them individually. Single fibrils joined each other over certain distances, demonstrating their meshlike network. From pH 9.3 (E) to 9.5 (F), parallel separated single long fibrils formed. From pH 9.7 to 10.3, (G, pH 9.7; H, pH 9.9; I, pH 10.1; and J, pH 10.3), single short fibrils oriented parallel, but separated from each other were observed. As before, the spacing between collagen fibrils increased with the pH. At pH 10.5 (K) and 10.7 (L), only few small fragments were observed. Absorption and imaging buffers contained 200 mM NaCl and 50 mM Tris–HCl. Full gray level of topographs correspond to a vertical scale of 5 nm.

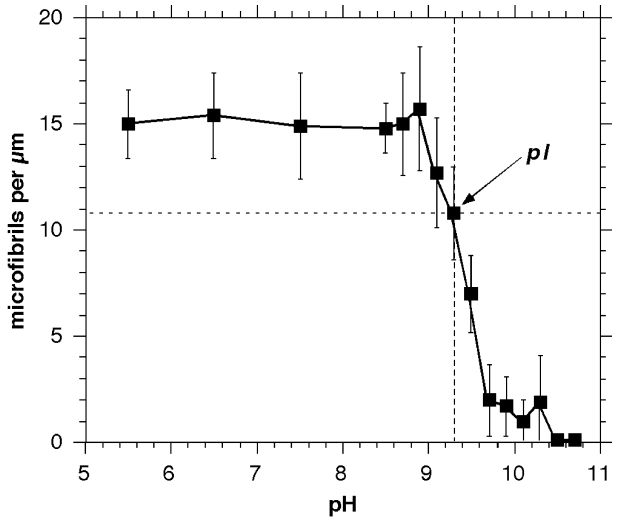

Fig. 3. Collagen fibrils per unit length of 1 μm. Values are given for pH values between 5 and 10.7 at an electrolyte concentration of 200 mM NaCl. Average of 80 measurements and their standard deviations are shown. The p*I* value of collagen I being 9.3 was pointed out (arrow).

odicity of 65.3 ± 2.7 nm (n = 50). Further addition of 5 mM $MgCl_2$ to the buffer solution did not change the overall appearance of the fibrils forming the monolayer nor did it influence the repeat of the periodic pattern (Fig. 4I).

3.5. Collagen assembly in buffer solutions mimicking cellular environments

In phosphate-buffered saline (PBS) at pH 7.4 and containing 200 mM NaCl, the collagen molecules assembled into fibrils that covered the supporting surface. This ultrathin matrix (Fig. 5A) was similar to that observed before under various conditions (Figs. 1, 2 and 4). The fibrils protruded 3.2 ± 0.4 nm (n = 120) above the supporting mica surface. Higher magnification topographs (Fig. 5B) showed that these fibrillar monolayers frequently contained elongated holes. The width of the holes varied from 50 to 300 nm while their lengths extended to more than 1500 nm.

In a buffer solution mimicking the cytoplasmic environment of a eukaryotic cell (Patton et al., 1989), the collagen molecules again assembled into pronounced fibrils (Fig. 5C). The fibrils protruded by about 3.8 ± 0.5 nm (n = 100) above the mica surface and exhibited a width (FWHM) varying between 5 (Fig. 5D; circle) and 650 nm. As observed before, individual fibrils laterally joined various other fibrils thereby forming a nanoscopic network. This network of had a pronounced longitudinal repeat of 66.0 ± 1.9 nm (average ± SD; n = 215) (Fig. 5D). The height modulation of the repeated protrusions was ~0.5 nm and did not depend on the width of fibrillar structures.

In a buffer solution mimicking a typical extracellular environment of a eukaryotic cell, the collagen molecules again assembled into pronounced fibrillar structures aligned in the direction of the hydrodynamic flow (Fig. 5E). The meshlike network of fibrils was similar to that observed for the assembly in cytoplasmic buffer (Fig. 5C) and had a similar longitudinal repeat of 66.0 ± 2.1 nm (n = 163) (Fig. 5F).

4. Discussion

We have developed methods to coat a non-biological surface with an ultrathin (~3 nm) well-oriented layer of collagen. We have shown that the density and orientation of the molecules making up this surface layer depend critically on the pH and the type of electrolyte in the buffer solution. Though effects of buffer conditions on the in vitro assembly of collagen have been noted before (Hattori et al., 1999; Suzuki et al., 1999; Wood and Keech, 1960), the very high spatial resolution obtained using AFM in the present study provides significant new insight into the molecular mechanism of collagen self-assembly.

Systematically characterizing these conditions provided possibilities to control the collagen self-assembly on a molecular scale. Besides the alignment of collagen fibrils, their spacing as well as the formation of their nanoscopic network could be adjusted by sample preparation conditions. Our results directly demonstrate the plasticity and variety of collagen assemblies. Furthermore, they provide insight into self-assembly mechanisms of collagen by which the ECM may be organized in vivo (Guidry and Grinnell, 1985; Harris et al., 1981; Lee et al., 1994).

4.1. Microribbons—a new assembly of collagen

High-resolution AFM topographs allowed detailed analysis of the assembly of collagen molecules into fibrillar structures (Figs. 1, 2, and 4). The smallest cross-section of collagen fibrils observed in this study was 3 × 5 nm. Because this matches the dimension of a single collagen microfibril that has been hypothesised to form the building block of collagen fibers (Hulmes, 2002; Orgel et al., 2001) we postulate that our smallest collagen fibrils represent single microfibrils. Because the thickness of our fibrillar structures was invariant (~3 nm) and did not depend on the width, which varied from 5 to more than 650 nm, we further postulate that our fibrils are formed by the lateral association of microfibrils. A 650-nm wide structure would therefore correspond to the lateral assembly of over 100 microfibrils. From now on, we will call these two dimensional structures microribbons and refer to the surface coating as a monolayer, because the average height of these microribbons corresponds to the diameter of one microfibril.

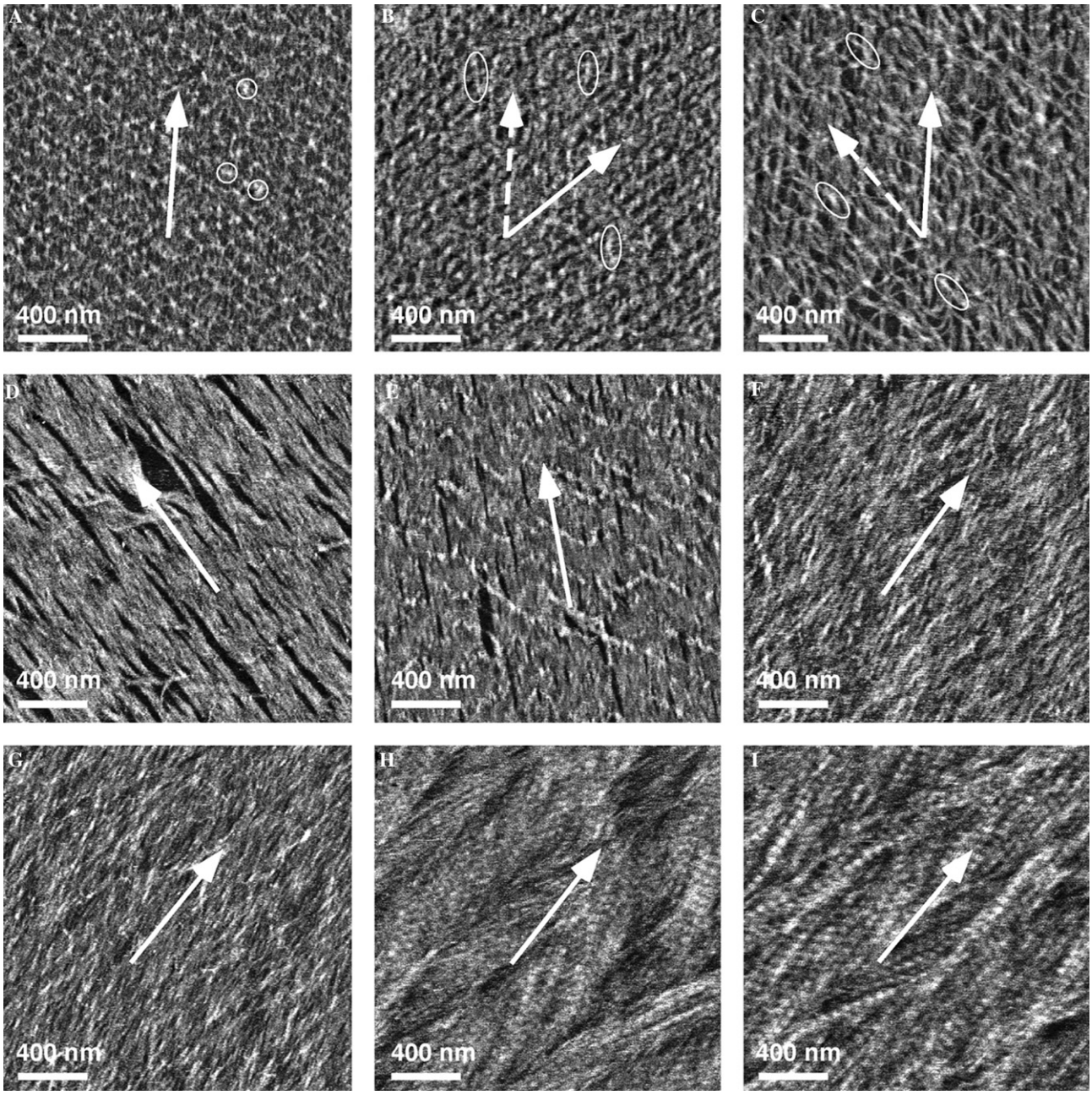

Fig. 4. Electrolyte dependent self-assembly of collagen. In all electrolytes used 10 mM $MgCl_2$ (A) 50 mM NaCl; (B) 100 mM NaCl; (C) 200 mM NaCl; (D) 200 mM NaCl; 5 mM $MgCl_2$; (E) 50 mM KCl; (F) 100 mM KCl; (G) 200 mM KCl; (H) 200 mM KCl; and 5 mM $MgCl_2$ (I) the collagen molecules assembled into fibrils which formed flat sheets. Arrows indicate the direction of the fibrils within these sheets. In case of (A), (B), and (C) a second layer of collagen fibrils was established onto the underlying collagen sheet, which was directly attached to the mica surface. Fibrils of this second layer had an angular orientation of $\sim 57 \pm 8°$ relative to the fibrils under lying collagen sheet. Surprisingly, the fibrillar density of this second layer was less than that observed for the underlying collagen layer. When adsorbed in KCl (F, G, and H), the collagen fibrils were twisted around each other forming a rougher pattern. At a KCl concentration above 200 mM (H), the collagen fibrils showed a longitudinal periodicity of 65.3 ± 2.7 nm. Adding small amounts of $MgCl_2$ to the monovalent electrolytes (E and I) did not influence the collagen self-assembly. All absorption buffers had a pH 7.5 (50 mM Tris–HCl). Full gray level of topographs corresponds to a vertical scale of 5 nm.

4.1.1. Microfibrillar spacing yields higher at pH approaching pI value

The p*I* value of the supporting mica surface is ~6 (Marti et al., 1995). However, neither the microfibrillar density nor the structural appearance changed within a pH ranging from 4.5 to 8.9. Thus, it is concluded that the assembly of collagen into microfibrils was not significantly influenced by the p*I* of mica. This finding is surprising because it is usually assumed that properties of the supporting surface significantly influence self-assembly of adsorbing

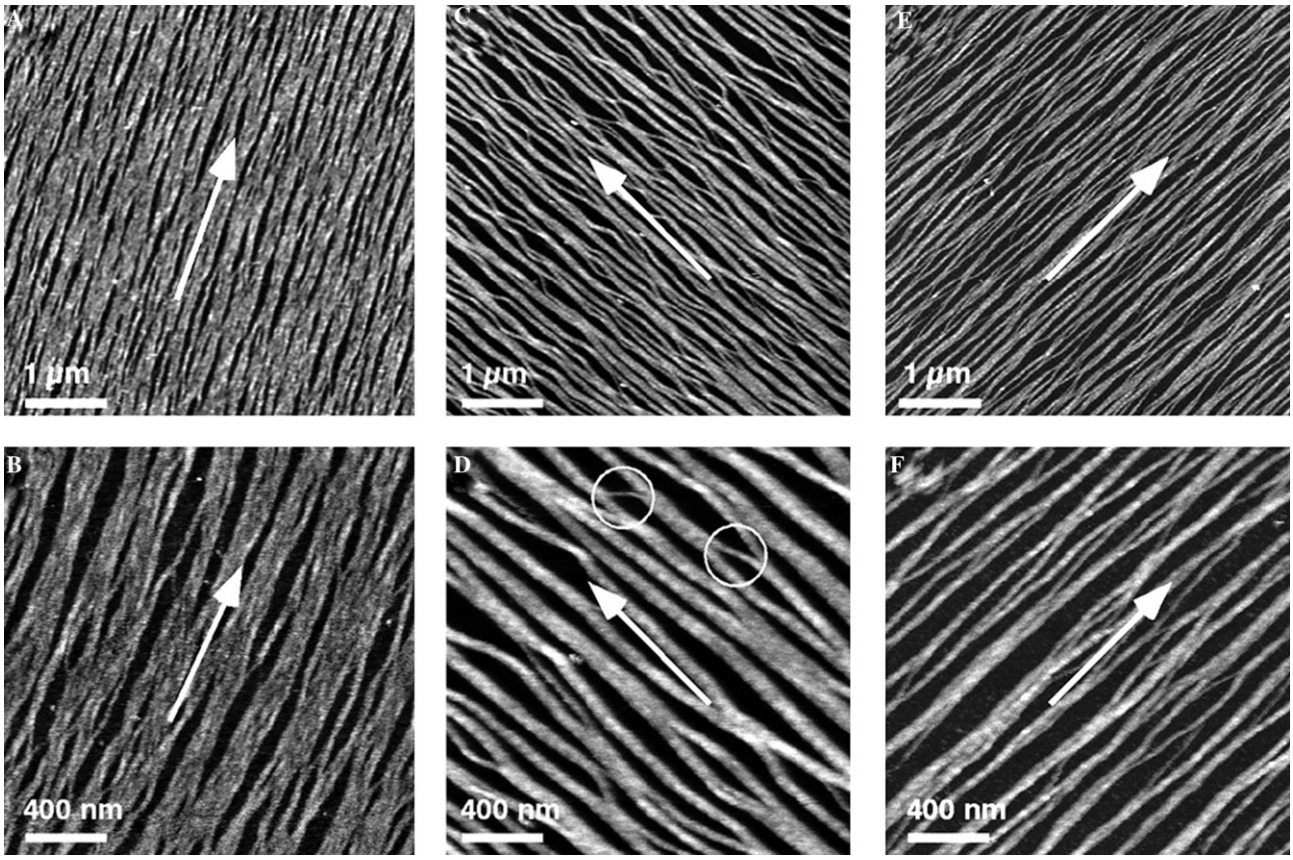

Fig. 5. Self-assembly of collagen in solutions mimicking different cellular environments. (A and B), Collagen fibrils assembled on to freshly cleaved mica in phosphate-buffered saline (PBS, 1.54 mM KH_2PO_4, and 2.71 mM Na_2HPO_4, pH 7.4) containing 200 mM NaCl. Collagen fibrils were aligned parallel to each other covering the supporting surface almost entirely. (C and D) Collagen fibrils assembled in buffer solution mimicking a typical cytoplasmic solution of an eukaryotic cell (130 mM monopotassium glutamate, 8.5 mM monosodium glutamate, 10 mM Hepes, 2 mM $MgCl_2$, 1 mM Na_2ATP, 1 mM EGTA, 0.5 mM NaH_2PO_4, 0.5 mM Na_2HPO_4, and 0.5 mM $CaCl_2$, pH 7.2 adjusted with KOH). The fibrils established the characteristic longitudinal period of 66.0 ± 1.9 nm such as typically observed for collagen I fibrils of tendon and tissue. (E and F) Collagen fibrils assembled in buffer solution mimicking a typical extracellular environment of an eukaryotic cell (109.2 mM NaCl, 4.1 mM KCl, 1.7 mM $CaCl_2$, 0.65 mM $MgCl_2$, 7.9 mM monosodium glutamate, 0.4 mM NaH_2PO_4, 0.3 mM Na_2HPO_4, 27 mM $NaHCO_3$, and 20 mM Hepes, pH 7.4 adjusted with NaOH). Again the fibrils exposed a characteristic longitudinal period of 66.0 ± 2.3 nm. In the topographs the width of the fibrils varied from 8 to 284 nm (measured at FWHM), while their height above the mica was 2.7 ± 0.3 nm ($n = 100$). Full gray level of topographs corresponds to a vertical scale of 5 nm.

molecules (Chakraborty and Golumbfskie, 2001; Jeong and Gutowska, 2002). Such interfacial influences, however, were not observed in this work.

In contrast to the supporting surface, the p*I* value of collagen I molecules lies at 9.3 (Hattori et al., 1999). The microfibrillar spacing increased at pH values above 8.9 and dropped to half of its maximum value at pH 9.3. Thus, we suggest that the pH dependent increase of collagen spacing is related to the isoelectric point of collagen. However, the isoelectric point determined by conventional methods rather represents a macroscopic measure of all molecular charges, though there may still exist local regions of the collagen molecule exposing high charge densities. Our observations of the gradually increasing separation between the collagen microfibrils suggest that they repel each other at pH close and above the p*I* value of the collagen molecules. Further investigations may focus on the underlying molecular mechanisms inducing collagen molecules to separate at pH values close to 9.3. Such insight will help to further understand the molecular interactions directing collagen molecules into their fibrillar assembly (Hulmes, 2002; Kadler et al., 1996).

4.1.2. Influence of electrolytes on the collagen assembly

In the presence of every electrolyte tested and at neutral pH, the collagen molecules assembled into microfibrils (Fig. 5). The microfibrils formed a monolayer, which almost completely covered the supporting mica surface. However, at electrolyte concentrations of 10 mM $MgCl_2$ (Fig. 5A), 50 mM NaCl (Fig. 5B) and 100 mM NaCl (Fig. 5C) a second layer of collagen molecules formed on top of the microfibrillar monolayer. This second collagen layer was most pronounced at electrolyte concentrations of 50 and 100 mM NaCl. The density of this layer was much lower than that of the

first layer. By further enhancing the electrolyte concentration to 200 mM NaCl (Fig. 5D), the second collagen layer almost disappeared. It is also interesting that the second monolayer did not form if NaCl was substituted using KCl. These experiments demonstrate that the self-assembly of collagen molecules into microfibrils and the formation of microfibrillar networks depend in a sensitive way on the electrolyte and its concentration.

Interestingly, the formation of a second collagen layer was not observed using buffer solutions mimicking different environments of eukaryotic cells and PBS (Fig. 5). This supports the above observation that the second layer of collagen molecules is only established within a distinct range of electrolyte concentrations. Comparing the electrolyte composition of the buffer solutions tested indicates that the assembly of a second collagen layer is inhibited by potassium ions. Because the second collagen layer was not observed in physiological relevant buffer solutions (Fig. 5), this form of assembly may not occur in vivo. However, it is not excluded that other cellular environments not mimicked in this work support such a sandwich-like assembly of collagen molecules into multilayered sheets. It will be interesting to test various physiological conditions mimicking other cellular environments and to characterize the collagen assembly in vitro and in vivo.

4.1.3. Microfibrils require certain conditions to establish periodic patterns

Collagen molecules self-assembled into two different supramolecular networks onto a supporting surface. In the first network, the collagen microfibrils exhibited a high degree of parallel alignment relative to each other. The microfibrils mainly associated laterally thereby forming flat bands or microribbons. If assembled in the absence of potassium, the surfaces of the microfibrils were smooth along their length and did not display any longitudinal patterns. This situation changed, however, as soon as potassium was present during the collagen assembly. In presence of potassium ions (Fig. 5), collagen microfibrils and microribbons formed a pattern with a period of ~66 nm. This value lies well within the characteristic values of 64–67 nm observed more than 60 years ago by electron microscopy (Schmitt et al., 1942, 1953) and by X-ray diffraction (Bear, 1942, 1944) for much thicker collagen fibers. (Suzuki et al., 1999) suggested that the longitudinal spacing of collagen fibrils depends on the lateral interaction between the collagen molecules. It was postulated that if the interactions were too strong, then the collagen molecules would assemble randomly between the nearest possible interaction sites, which would result in a loss of the characteristic fibril periodicity. If the interactions were weaker, then the molecules could find preferred, periodic interaction sites, giving rise to the cross-striations.

4.1.4. Microfibrils can establish periodic patterns by lateral assembly

The discussion of collagen fibril assembly includes the question how microfibrils assemble into the final fibril. Recent attempts to visualize isolated microfibrils have not been totally convincing, although it has been shown that microfibrils exist in native fibrils (Hulmes, 2002; Orgel et al., 2001). The AFM topographs show that microfibrils assemble laterally to form microribbons. Under certain preparation conditions (pH and electrolyte), our AFM data directly provides evidence of a longitudinal D repeat in transverse section of isolated microfibrils and of microribbons (Fig. 5). This repeat has been observed from fibrils being hundreds of nanometer in diameter to their 4 nm thick building blocks (Miller and Parry, 1973). It was somehow surprising, that microfibrils, being the minimum filamentous structure, already posses the typical axial D repeat of tendon fibers (Hulmes, 2002), since other models for the molecular packing in 25 nm fibrils do not show any microfibrillar D repeat (Blaschke et al., 2000; Chapman, 1989).

The smallest microribbon showing a 65 nm periodicity had a width of only 10 nm (Fig. 5D; circle). Thus, two laterally assembled collagen microfibrils can create a D-period. This suggests that microribbons establish their characteristic D-period by lateral assembly of correctly aligned microfibrils. The periodic 0.5-nm-protrusions that define the 65-nm period were homogeneous over the entire width of the microribbon. This implies that microfibrils assemble into the broader ribbons by correct lateral registration, a mechanism suggested for microfibril assembly into thick collagen fibers of tendon (Hulmes, 2002; Kadler et al., 1996).

In previous work, solubilized collagen type I molecules were assembled in various buffer solutions and structurally investigated by electron microscopy (Hattori et al., 1999; Holmes et al., 1986; Perret et al., 2001; Sato et al., 2000; Suzuki et al., 1999; Wood and Keech, 1960) or AFM (Agarwal et al., 2002; Chernoff and Chernoff, 1992; Gale et al., 1995; Lin et al., 1999; Paige et al., 1998). The characteristic D-band periodicity of collagen was observed if the self-assembly took place in buffer solutions containing potassium. In agreement with our finding, the characteristic D-periodicity of collagen fibers was not observed if the buffer solution contained no potassium (Agarwal et al., 2002; Lin et al., 1999; Paige et al., 1998; Suzuki et al., 1999). It may be noted, that in most cases of these observations, the collagen molecules assembled into much thicker fibers (~100 nm or more) than observed here by AFM.

4.1.5. Different ways of microfibril assembly

Another interesting mechanism of collagen self-assembly was seen in buffer solutions containing more than 100 mM KCl (Figs. 4F–I). The collagen molecules formed microfibrils that exhibited an overall alignment,

but were somehow woven and twisted around each other. This observation was in contrast to the other measurements in which the microfibrils assembled laterally forming flat bands. At KCl concentrations above 200 mM these twisted microfibrillar bundles established the typical D-periodicity of collagen fibers.

5. Conclusion

Collagen type I can assemble microfibrils that join laterally to form two-dimensional bands. These structures, termed microribbons, have a thickness of ~3 nm, which corresponds to that of a single microfibril. It was found that the assembly of these microfibrils into a nanoscopic network depended critically on the pH and electrolyte composition of the buffer solution. Furthermore, the D-periodicity of microribbons required potassium ions in the buffer. Our novel observation of the assembly of collagen into microribbons provides interesting insights into collagen structure and assembly. The discovery of alternate collagen structures, which may exist in vivo, may offers novel ways to bio-functionalize surfaces.

Acknowledgments

The authors thank Khaled Khairy, Clemens Franz, Kate Poole, and David Cisneros for discussing of the manuscript. This work was supported by the Deutsche Forschungsgemeinschaft (DFG), the European Union (EU) and the state of Saxony.

References

Agarwal, G., Kovac, L., Radziejewski, C., Samuelsson, S.J., 2002. Binding of discoidin domain receptor 2 to collagen I: an atomic force microscopy investigation. Biochemistry 41, 11091–11098.

Akiyama, S.K., Nagata, K., Yamada, K.M., 1990. Cell surface receptors for extracellular matrix components. Biochim. Biophys. Acta 1031, 91–110.

Bear, R.S., 1942. Long X-ray diffraction spacings of collagen. J. Am. Chem. Soc. 64, 727–729.

Bear, R.S., 1944. X-study of the large fibre axis period of collagen. J. Am. Chem. Soc. 66, 1297–1301.

Bell, E., Ivarsson, B., Merrill, C., 1979. Production of a tissue-like structure by contraction of collagen lattices by human fibroblasts of different proliferative potential in vitro. Proc. Natl. Acad. Sci. USA 76, 1274–1278.

Bigi, A., Gandolfi, M., Roveri, N., Valdre, G., 1997. In vitro calcified tendon collagen: an atomic force and scanning electron microscopy investigation. Biomaterials 18, 657–665.

Bishop, P.N., 2000. Structural macromolecules and supramolecular organisation of the vitreous gel. Prog. Retin. Eye Res. 19, 323–344.

Blaschke, U.K., Eikenberry, E.F., Hulmes, D.J., Galla, H.J., Bruckner, P., 2000. Collagen XI nucleates self-assembly and limits lateral growth of cartilage fibrils. J. Biol. Chem. 275, 10370–10378.

Chakraborty, A.K., Golumbfskie, A.J., 2001. Polymer adsorption-driven self-assembly of nanostructures. Annu. Rev. Phys. Chem. 52, 537–573.

Chapman, J.A., 1989. The regulation of size and form in the assembly of collagen fibrils in vivo. Biopolymers 28, 1367–1382.

Chen, C.H., Hansma, H.G., 2000. Basement membrane macromolecules: insights from atomic force microscopy. J. Struct. Biol. 131, 44–55.

Chernoff, E.A.G., Chernoff, D.A., 1992. Atomic force microscope images of collagen-fibers. J. Vasc. Sci. Tech. 10, 596–599.

Coombes, A.G., Verderio, E., Shaw, B., Li, X., Griffin, M., Downes, S., 2002. Biocomposites of non-crosslinked natural and synthetic polymers. Biomaterials 23, 2113–2118.

Demers, L.M., Ginger, D.S., Park, S.J., Li, Z., Chung, S.W., Mirkin, C.A., 2002. Direct patterning of modified oligonucleotides on metals and insulators by dip-pen nanolithography. Science 296, 1836–1838.

Drake, B., Prater, C.B., Weisenhorn, A.L., Gould, S.A.C., Albrecht, T.R., Quate, C.F., Cannell, D.S., Hansma, H.G., Hansma, P.K., 1989. Imaging crystals, polymers, and processes in water with the atomic force microscope. Science 243, 1586–1588.

Engel, A., Müller, D.J., 2000. Observing single biomolecules at work with the atomic force microscope. Nat. Struct. Biol. 7, 715–718.

Gale, M., Pollanen, M.S., Markiewicz, P., Goh, M.C., 1995. Sequential assembly of collagen revealed by atomic force microscopy. Biophys. J. 68, 2124–2128.

Grinnell, F., 2000. Fibroblast-collagen-matrix contraction: growth-factor signalling and mechanical loading. Trends Cell Biol. 10, 362–365.

Grinnell, F., 2003. Fibroblast biology in three-dimensional collagen matrices. Trends Cell Biol. 13, 26426–26429.

Guidry, C., Grinnell, F., 1985. Studies on the mechanism of hydrated collagen gel reorganization by human skin fibroblasts. J. Cell. Sci. 79, 67–81.

Habelitz, S., Balooch, M., Marshall, S.J., Balooch, G., Marshall Jr., G.W., 2002. In situ atomic force microscopy of partially demineralized human dentin collagen fibrils. J. Struct. Biol. 138, 227–236.

Harris, A.K., Stopak, D., Wild, P., 1981. Fibroblast traction as a mechanism for collagen morphogenesis. Nature 290, 249–251.

Hattori, S., Adachi, E., Ebihara, T., Shirai, T., Someki, I., Irie, S., 1999. Alkali-treated collagen retained the triple helical conformation and the ligand activity for the cell adhesion via alpha 2 beta 1 integrin. J. Biochem. 125, 676–684.

Hohenester, E., Engel, J., 2002. Domain structure and organisation in extracellular matrix proteins. Matrix Biol. 21, 115–128.

Holmes, D.F., Capaldi, M.J., Chapman, J.A., 1986. Reconstitution of collagen fibrils in-vitro: the assembly process depends on the initiating procedure. Int. J. Biol. Macromol. 8, 161–166.

Hulmes, D.J., 2002. Building collagen molecules, fibrils, and suprafibrillar structures. J. Struct. Biol. 137, 2–10.

Hulmes, D.J., Jesior, J.C., Miller, A., Berthet-Colominas, C., Wolff, C., 1981. Electron microscopy shows periodic structure in collagen fibril cross sections. Proc. Natl. Acad. Sci. USA 78, 3567–3571.

Hulmes, D.J., Miller, A., 1981. Molecular packing in collagen. Nature 293, 234–239.

Jeong, B., Gutowska, A., 2002. Lessons from nature: stimuli-responsive polymers and their biomedical applications. Trends Biotechnol. 20, 305–311.

Jurvelin, J.S., Müller, D.J., Wong, M., Studer, D., Engel, A., Hunziker, E.B., 1996. Surface and sub-surface morphology of bovine humeral articular cartilage as assessed by atomic force- and transmission electron microscopy. J. Struct. Biol. 117, 45–54.

Kadler, K.E., 1993. Learning how mutations in type I collagen genes cause connective tissue disease. Int. J. Exp. Pathol. 74, 319–323.

Kadler, K.E., Holmes, D.F., Trotter, J.A., Chapman, J.A., 1996. Collagen fibril formation. Biochem. J. 316, 1–11.

Kunicki, T.J., 2002. The influence of platelet collagen receptor polymorphisms in hemostasis and thrombotic disease. Arterioscler. Thromb. Vasc. Biol. 22, 14–20.

Lee, C.H., Singla, A., Lee, Y., 2001. Biomedical applications of collagen. Int. J. Pharm. 221, 1–22.

Lee, J., Leonard, M., Oliver, T., Ishihara, A., Jacobson, K., 1994. Traction forces generated by locomoting keratocytes. J. Cell. Biol. 127, 1957–1964.

Lee, K.B., Park, S.J., Mirkin, C.A., Smith, J.C., Mrksich, M., 2002. Protein nanoarrays generated by dip-pen nanolithography. Science 295, 1702–1705.

Lin, H., Clegg, D.O., Lal, R., 1999. Imaging real-time proteolysis of single collagen I molecules with an atomic force microscope. Biochemistry 38, 9956–9963.

Lloyd, A.W., 2002. Interfacial bioengineering to enhance surface biocompatibility. Med. Device Technol. 13, 18–21.

Marshall, G.W., Yucel, N., Balooch, M., Kinney, J.H., Habelitz, S., Marshall, S.J., 2001. Sodium hypochlorite alterations of dentin and dentin collagen. Surf. Sci. 491, 444–455.

Marti, A., Hähner, G., Spencer, N.D., 1995. Sensitivity of frictional forces to pH on a nanometer scale: a lateral force microscopy study. Langmuir 11, 4632–4635.

Meller, D., Peters, K., Meller, K., 1997. Human cornea and sclera studied by atomic force microscopy. Cell Tissue Res. 288, 111–118.

Miller, A., Parry, D.A., 1973. Structure and packing of microfibrils in collagen. J. Mol. Biol. 75, 441–447.

Myllyharju, J., Kivirikko, K.I., 2001. Collagens and collagen-related diseases. Ann. Med. 33, 7–21.

Orgel, J.P., Miller, A., Irving, T.C., Fischetti, R.F., Hammersley, A.P., Wess, T.J., 2001. The in situ supermolecular structure of type I collagen. Structure (Camb) 9, 1061–1069.

Ottani, V., Martini, D., Franchi, M., Ruggeri, A., Raspanti, M., 2002. Hierarchical structures in fibrillar collagens. Micron 33, 587–596.

Paige, M.F., Rainey, J.K., Goh, M.C., 1998. Fibrous long spacing collagen ultrastructure elucidated by atomic force microscopy. Biophys. J. 74, 3211–3216.

Patton, H.D., Fuchs, A.F., Hille, B., Scher, A.M., Steiner, R., 1989. Textbook of Physiology. W.B. Saunders, Philadelphia.

Perret, S., Merle, C., Bernocco, S., Berland, P., Garrone, R., Hulmes, D.J., Theisen, M., Ruggiero, F., 2001. Unhydroxylated triple helical collagen I produced in transgenic plants provides new clues on the role of hydroxyproline in collagen folding and fibril formation. J. Biol. Chem. 276, 43693–43698.

Prockop, D.J., 1998. What holds us together? Why do some of us fall apart? What can we do about it? Matrix Biol. 16, 519–528.

Prockop, D.J., 1999. Hopkins memorial medal lecture. Pleasant surprises en route from the biochemistry of collagen to attempts at gene therapy. Biochem. Soc. Trans. 27, 15–31.

Prockop, D.J., Fertala, A., 1998. The collagen fibril: the almost crystalline structure. J. Struct. Biol. 122, 111–118.

Raspanti, M., Alessandrini, A., Ottani, V., Ruggeri, A., 1997. Direct visualization of collagen-bound proteoglycans by tapping-mode atomic force microscopy. J. Struct. Biol. 119, 118–122.

Raspanti, M., Congiu, T., Guizzardi, S., 2001. Tapping-mode atomic force microscopy in fluid of hydrated extracellular matrix. Matrix Biol. 20, 601–604.

Raspanti, M., Congiu, T., Guizzardi, S., 2002. Structural aspects of the extracellular matrix of the tendon: an atomic force and scanning electron microscopy study. Arch. Histol. Cytol. 65, 37–43.

Revenko, I., Sommer, F., Minh, D.T., Garrone, R., Franc, J.M., 1994. Atomic force microscopy study of the collagen fibre structure. Biol. Cell. 80, 67–69.

Sato, K., Ebihara, T., Adachi, E., Kawashima, S., Hattori, S., Irie, S., 2000. Possible involvement of aminotelopeptide in self-assembly and thermal stability of collagen I as revealed by its removal with proteases. J. Biol. Chem. 275, 25870–25875.

Schmitt, F., Gross, J., Highberger, J., 1953. A new particle type in certain connective tissue extracts. Proc. Natl. Acad. Sci. USA 39, 459–470.

Schmitt, F.O., Hall, C.E., Jakns, M.A., 1942. Electron microscopy investigations of the structure of collagen. J. Cell. Comp. Physiol. 20, 11–13.

Squire, J.M., Freundlich, A., 1980. Direct observation of a transverse periodicity in collagen fibrils. Nature 288, 410–413.

Sun, H.B., Smith, G.N., Hasty, K.A., Yokota, H., 2000. Atomic force microscopy-based detection of binding and cleavage site of matrix metalloproteinase on individual type II collagen helices. Anal. Biochem. 283, 153–158.

Suzuki, Y., Someki, I., Adachi, E., Irie, S., Hattori, S., 1999. Interaction of collagen molecules from the aspect of fibril formation: acid-soluble, alkali-treated, and MMP1-digested fragments of type I collagen. J. Biochem. (Tokyo) 126, 54–67.

Thalhammer, S., Heckl, W.M., Zink, A., Nerlich, A.G., 2001. Atomic force microscopy for high resolution imaging of collagen fibrils—A new technique to investigate collagen structure in historic bone tissues. J. Arch. Sci. 28, 1061–1068.

Wood, G.C., Keech, M.K., 1960. Formation of fibrils from collagen solutions. 1. Effect of experimental conditions—kinetic and electron-microscope studies. Biochem. J. 75, 588–598.